Dyes and Pigments 86 (2010) 190–196

Contents lists available at ScienceDirect

Dyes and Pigments

journal homepage: www.elsevier.com/locate/dyepig

The synthesis and photoluminescence characteristics of novel blue light-emitting naphthalimide derivatives

Yi Wang [a], Xiaogen Zhang [a], Bing Han [b], Junbiao Peng [b], Shiyou Hou [a], Yan Huang [a,*], Huiqin Sun [c], Minggui Xie [a], Zhiyun Lu [d,*]

[a] College of Chemistry, Sichuan University, Chengdu 610064, PR China
[b] Institute of Polymer Optoelectronic Materials and Devices, South China University of Technology, Guangzhou 510640, PR China
[c] Analytical and Testing Center, Sichuan University, Chengdu 610064, PR China
[d] Key Laboratory of Green Chemistry and Technology, Minister of Education, Sichuan University, Chengdu 610064, PR China

ARTICLE INFO

Article history:
Received 10 October 2009
Received in revised form
7 January 2010
Accepted 8 January 2010
Available online 18 January 2010

Keywords:
1,8-Naphthalimide
Synthesis
Blue light-emission
Photoluminescence
Fluorescence quantum yield
Electron affinity

ABSTRACT

Substitution at the 4-position of 1,8-naphthalimide with electron-donating phenoxy or *tert*-butyl modified phenoxy groups, novel naphthalimide derivatives were obtained which emitted blue fluorescence with emission peaks of 425–444 nm in chloroform solution under UV irradiation, with highest relative photoluminescence quantum efficiency of 0.82. When in solid film, only compounds that contained *ortho*-*tert*-butylphenoxy substituents displayed blue photoluminescence of 438–451 nm, with highest absolute fluorescence quantum yield of 0.29; whereas other compounds showed greenish blue fluorescence at 471–478 nm, with highest absolute fluorescence quantum yield of 0.42. Cyclic voltammetry studies revealed that the molecules have low-lying energy levels of the lowest unoccupied molecular orbital (LUMO) ranging from −3.29 eV to −3.24 eV, and energy levels of the highest occupied molecular orbital (HOMO) ranging from −6.26 eV to −6.16 eV, suggesting they may possess good electron-transporting or hole-blocking properties. The findings indicate that the molecules offer potential as dopants as well as non-doping light-emitting materials with good electron injection capabilities for fabrication of blue or greenish blue organic light-emitting diodes.

1. Introduction

Owing to their potential application in flat panel displays and solid-state light sources, the development of organic light-emitting diode (OLED) materials has attracted much attention over the past twenty or so years. In the context of full-colour OLEDs, efficient blue emitters are of especial interest because blue OLEDs display much poorer performance compared to red and green emitters [1–5]. The luminous efficiency of a blue OLED with CIE x,y coordinates of 0.16, 0.12, respectively, is only 1.57 lm W^{-1} [6], while that of green emitter is 26.2 lm W^{-1}[1]. Moreover, as concentration quenching is a common characteristic of fluorescent dyes, a doping procedure is generally employed during the fabrication of OLEDs [1,2,7,8]. However, this procedure results in poor device durability, as the dopants may aggregate, stack, and crystallize, resulting in phase separation under prolonged electric stress and at high working temperatures [3,9]. Therefore, intense research efforts have focused on the development of non-doped, pure blue light-emitting materials with high fluorescence quantum yield in solid states.

Among the various kinds of OLED emitters, 1,8-naphthalimide derivatives have attracted much attention owing to their good optical, thermal and chemical stabilities, as well as high photoluminescence (PL) quantum efficiency in solution [10–13]. By introducing different electron-donating substituents, such as *N*-substituted groups [14,15], *C*-substituted groups [16–18], and *O*-substituted groups [19], in the 4-position of 1,8-naphthalimides, their PL emission colour can be readily tuned from yellowish green to pure blue. Furthermore, it has been reported that naphthalimide derivatives generally have high electron affinity due to the existence of an electron-deficient centre [20–24] and should display good electron-transporting or hole-blocking capabilities that are appropriate for balanced carrier injection in OLEDs.

By employing naphthalimide derivatives as emitters, efficient OLEDs have been obtained [13,14,25–29], such emitters having employed *C*-substituted groups (eg arylalkynyl [28], arylalkenyl [29]) or *N*-substituted groups (eg arylamino [14], alkylamino [26]) in the 4-postion and electroluminescence (EL) colours varying

* Corresponding authors. Tel.: +86 28 85410059; fax: +86 28 85413601.
E-mail addresses: huangyan@scu.edu.cn (Y. Huang), luzhiyun@scu.edu.cn (Z. Lu).

0143-7208/$ – see front matter © 2010 Elsevier Ltd. All rights reserved.
doi:10.1016/j.dyepig.2010.01.003

from greenish blue to orange have been secured. Although it is reported that 4-alkyloxy or 4-aryloxy substituted naphthalimides exhibit pure blue fluorescence in solution [19,30], there is, to our knowledge, only one report employing such kind of naphthalimide, *i.e.*, 4,5-diethoxy-1,8-naphthalimide, as EL material [31]. The dye gives pure blue PL emission at 460 nm, but shows green EL peak at 520 nm, and the performance of the OLED is quite poor (35 cd m^{-2} at 100 mA cm^{-2}). The red-shifted EL emission as well as the low device efficiency may be ascribed to the concentration quenching of the planar dyes caused by aggregation and close stacking.

In order to exploit blue emitters with reduced propensity of concentration quenching, rigid phenoxy substituents were introduced into the 4-position of naphthalimides [19,32], and *tert*-butyl substituents were introduced at different positions of the phenoxy groups to achieve more bulky molecules and alter the conjugation length as well. In this work, as it has been reported that H-bonds can be formed between hydroxy and carbonyl groups in *N*-(2-hydroxyethyl)-1,8-naphthalimide [33], the influence that H-bonds may have on photophysical characteristics has been investigated by modifying the carboximide site with *N*-(2-hydroxyethyl) or *N*-(2-acetoxyethyl) substituents.

2. Experimental

2.1. Materials and instrumentation

All chemicals were purchased from Aldrich and Acros Chemical Co., and were used without further purification. The solvents were of analytical grade and freshly distilled before use. *N*, *N*-dimethylformamide (DMF) and dimethylsulfoxide (DMSO) were dried with CaH_2 and freshly distilled before use.

^1H NMR and ^{13}C NMR spectra were recorded on a BRUKER (AVII-400) spectrometer in $CDCl_3$ using TMS as internal standard. High resolution TOF-MS spectra were recorded on a Waters Q-TOF-Premiter instrument. UV–vis absorption spectra of the 10^{-5} mol L^{-1} solutions as well as spin-coated films on quartz plates were collected with a UV–visible spectroscopy (HP8453A from Agilent Co.). Photoluminescence spectra were recorded with a CCD spectrography (INTRASPEC IV from Oriel Co.). Relative PL efficiencies in chloroform solution were determined by using 10^{-5} mol L^{-1} quinine sulfate in 0.1 mol L^{-1} H_2SO_4 ($\varphi = 0.55$) as the standard with a fluorescence spectrophotometer (F-7000 from Hitachi), while absolute PL quantum yields in neat films were determined with an integrating sphere (IS80 form Labsphere) equipped together with a digital photometer (S370 from UDT). In the measurement of PL spectra and PL efficiencies, different excitations were chosen under the guidance of absorbance peaks to assure enough absorption. All the thin films were prepared by the following procedure: the samples were dissolved in chloroform with the concentration of 40 mg mL^{-1}, then spin-coated onto quartz substrates at a speed of 1700 rpm, the thickness of the films was about 100 nm. Melting points were measured by a differential scanning calorimeter (DSC200PC from NETZSCH). The cyclic voltammograms reported here were recorded with a CHI830B electrochemical workstation at a constant scan rate of 50 mV s^{-1}. The measurements were performed in 1 mmol L^{-1} acetonitrile solutions of the samples with tetrabutylammonium hexafluorophosphate solution (0.1 mol L^{-1} in acetonitrile) as supporting electrolyte at room temperature. The cyclic voltammetric system was constructed using a three-electrode undivided electrochemical cell consisted of a Pt working electrode, a Pt-wire counter electrode, and a $Ag/AgNO_3$ reference electrode (0.1 mol L^{-1} in CH_3CN) under protection of nitrogen, and each measurement was calibrated with an internal standard, ferrocene/ferrocenium redox system [34].

2.2. Syntheses

The synthetic route to the target molecules is shown in Fig. 1. Intermediate 2 was prepared according to the reported procedure [35]. Compounds 3a–3d were prepared *via* nucleophilic substitution reactions of phenol and substituted phenols with 2; compounds 4a–4d were obtained by further acetylation of 3a–3d.

2.2.1. 4-Phenoxy-N-(2-hydroxyethyl)-1,8-naphthalimide (3a)

To a solution of 0.32 g intermediate 2 (1.0 mmol) dissolved in 40 mL of anhydrous DMF were added phenol 0.20 g (2 mmol) and anhydrous potassium carbonate 0.54 g (4 mmol). The mixture was stirred at 100 °C for 90 min under protection of nitrogen, after the reactant was cooled down, 40 mL of water was added, the yellow precipitate was collected and purified by column chromatograph (eluent: petroleum ether/ethyl acetate = 2/1) to afford pale yellow solid. Yield: 75.7%. Mp: 157–158 °C; ^1H NMR (400 MHz, $CDCl_3$)δ (ppm): 8.74(d, J = 8.0 Hz, 1H), 8.67(d, J = 7.2 Hz, 1H), 8.46(d,

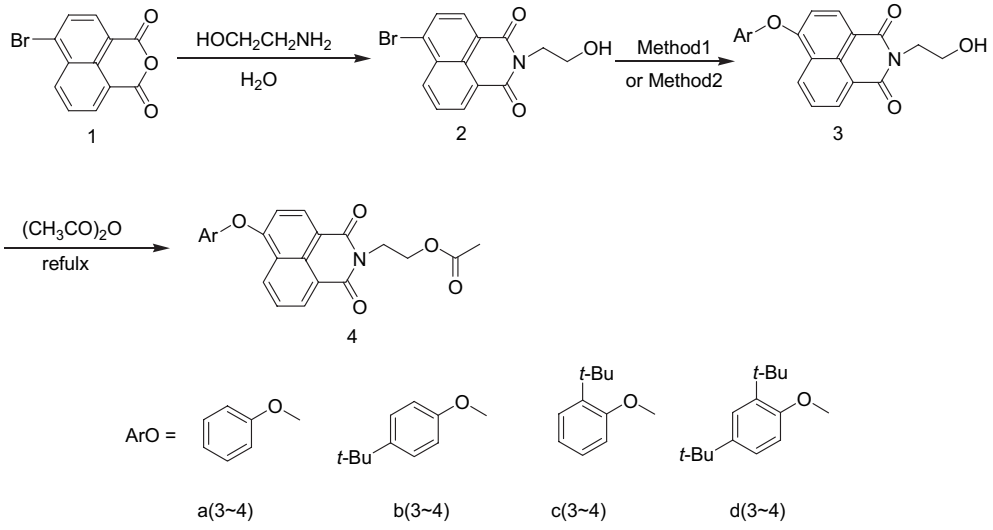

Fig. 1. The synthetic route to naphthalimide derivatives (Method1: DMF/K_2CO_3; Method2: DMSO/KOH).

J = 8.4 Hz, 1H), 7.80(t, J = 8.0 Hz, 1H), 7.50(t, J = 8.0 Hz, 2H), 7.32 (t, J = 7.2 Hz, 1H), 7.20(d, J = 8.0 Hz, 2H), 6.91(d, J = 8.0 Hz, 1H), 4.46 (t, J = 5.2 Hz, 2H), 3.99(t, J = 5.2 Hz, 2H); ^{13}C NMR (100 MHz, $CDCl_3$) δ(ppm): 165.25, 164.65, 160.21, 154.67, 133.22, 132.20, 130.45, 129.73, 128.93, 126.52, 125.72, 123.87, 122.27, 120.84, 116.13, 110.51, 61.95, 42.77; TOF-MS: m/z 334.1062 (M+1), Calc. for M_W: 334.1079.

2.2.2. 4-Phenoxy-N-(2-acetoxyethyl)-1,8-naphthalimide (4a)

0.48 g (1.3 mmol) 3a was mixed with 25 mL of acetic anhydride and stirred at 130 °C for 2 h. After the reactant was cooled down, the pale yellow precipitate was filtered and recrystallized from ethanol to afford pale yellow solid. Yield: 67.0%. Mp: 177–178 °C; ^{1}H NMR (400 MHz, $CDCl_3$)δ(ppm): 8.74–8.72 (m, 1H), 8.69–8.67 (m, 1H), 8.47(d, J = 8.4 Hz, 1H), 7.82–7.78 (m, 1H), 7.52–7.48 (m, 2H), 7.32 (t, J = 7.6 Hz, 1H), 7.20 (d, J = 7.6 Hz, 2H), 6.92 (d, J = 8.4 Hz, 1H), 4.49 (t, J = 5.2 Hz, 2H), 4.43 (t, J = 5.2 Hz, 2H), 2.02(s, 3H); ^{13}C NMR (100 MHz, $CDCl_3$)δ(ppm): 170.96, 164.43, 163.76, 160.04, 154.84, 132.97, 132.03, 130.42, 129.83, 128.77, 126.51, 125.62, 124.04, 122.44, 120.76, 116.37, 110.65, 61.68, 38.98, 29.68; TOF-MS: m/z 376.1211(M+1), Calc. for M_W: 376.1185.

2.2.3. 4-[(4-tert-butylphenoxy)]-N-(2-hydroxyethyl)-1,8-naphthalimide (3b)

Compound 3b was synthesized with the same procedure as 3a, using 4-*tert*-butylphenol and 2 as starting materials. Yield: 54.0%. Mp: 174–175 °C. ^{1}H NMR (400 MHz, $CDCl_3$)δ(ppm): 8.76–8.73(m, 1H), 8.69–8.67(m, 1H), 8.47(d, J = 8.4 Hz, 1H), 7.80(t, J = 8.0 Hz, 1H), 7.51–7.48(m, 2H), 7.14–7.11(m, 2H), 6.93(d, J = 8.0 Hz, 1H), 4.47(t, J = 5.2 Hz, 2H), 3.99(t, J = 5.2 Hz, 2H), 1.38(s, 9H); ^{13}C NMR (100 MHz, $CDCl_3$)δ(ppm): 164.30, 163.71, 159.52, 151.10, 147.79, 132.29, 131.16, 128.71, 128.00, 126.25, 125.41, 122.81, 121.21, 119.28, 114.83, 109.22, 61.02, 41.76, 33.58, 30.44, 28.67; TOF-MS: m/z 390.1693 (M+1), Calc. for M_W: 390.1705.

2.2.4. 4-[(4-tert-butylphenoxy)]-N-(2-acetoxyethyl)-1,8-naphthalimide (4b)

Compound 4b was synthesized with the same procedure as 4a, using 3b and acetic anhydride as reactants. Yield: 76.0%. Mp: 154–155 °C. ^{1}H NMR (400 MHz, $CDCl_3$)δ(ppm): 8.74 (d, J = 8.0 Hz, 1H), 8.68 (d, J = 7.2 Hz, 1H), 8.47 (d, J = 8.4 Hz, 1H), 7.79 (t, J = 8.0 Hz, 1H), 7.51–7.48 (m, 2H), 7.13–7.10 (m, 2H), 6.93 (d, J = 8.4 Hz, 1H), 4.49 (t, J = 5.2 Hz, 2H), 4.43 (t, J = 5.2 Hz, 2H), 2.01 (s, 3H), 1.38 (s, 9H); ^{13}C NMR (100 MHz, $CDCl_3$)δ(ppm): 171.02, 164.50, 163.83, 160.40, 152.22, 148.76, 133.07, 132.02, 129.80, 128.87, 127.26, 126.42, 123.94, 122.36, 120.27, 116.03, 110.30, 61.69, 38.95, 34.60, 31.47, 20.88; TOF-MS: m/z: 432.1823 (M+1), Calc. for M_W: 432.1811.

2.2.5. 4-(2-tert-butylphenoxy)-N-(2-hydroxyethyl)-1,8-naphthalimide (3c)

To a solution of 2-*tert*-butylphenol 0.75 g (5 mmol) in 20 mL of anhydrous DMSO was added 0.35 g (6.25 mmol) potassium hydroxide. The resulting mixture was stirred at room temperature for 30 min under protection of nitrogen, then a solution of 0.80 g (2.5 mmol) 2 dissolved in 20 mL DMSO was added dropwise over 30 min. The mixture was stirred at room temperature for 3 h, neutralized to pH = 7 by 1 mol L^{-1} hydrochloric acid, and then extracted with 20 mL × 3 ethyl acetate. The organic layer was washed with water, dried under anhydrous magnesium sulfate, then vacuum-vaporized to remove solvent. The residue was purified by column chromatograph (petroleum ether/ethyl acetate = 8/1) to obtain pale yellow solid. Yield: 41.2%, Mp: 179–180 °C. ^{1}H NMR (400 MHz, $CDCl_3$)δ(ppm): 8.76 (d, J = 8.4 Hz, 1H), 8.70 (d, J = 7.2 Hz, 1H), 8.48 (d, J = 8.0 Hz, 1H), 7.83 (t, J = 8.0 Hz, 1H), 7.54–7.48 (m, 1H), 7.29–7.25 (m, 2H), 7.01–6.98 (m, 1H), 6.91(d, J = 8.4 Hz, 1H), 4.47 (t, J = 5.2 Hz, 2H), 3.98 (t, J = 5.2 Hz, 2H), 1.41 (s, 9H); ^{13}C NMR (100 MHz, $CDCl_3$)$\delta\delta$(ppm): 165.25, 164.66, 160.31, 153.38, 142.11, 132.21, 131.16,129.87, 128.91, 126.64, 125.60, 124.15, 122.44, 122.02, 115.94, 110.80, 61.97, 42.86, 34.83, 30.42, 29.68 ; TOF-MS: m/z 390.1693 (M+1), Calc. for M_W: 390.1705.

2.2.6. 4-(2-tert-butylphenoxy)-N-(2-acetoxyethyl)-1,8-naphthalimide (4c)

Compound 4c was synthesized with the same procedure as 4a, using 3c and acetic anhydride as starting materials. Yield: 72.0%, Mp: 96–98 °C. ^{1}H NMR (400 MHz, $CDCl_3$)δ(ppm): 8.76–8.74(m, 1H), 8.70–8.68(m, 1H), 8.48(d, J = 8.4 Hz, 1H), 7.84–7.80(m, 1H), 7.55–7.53(m, 1H), 7.30–7.28(m, 1H), 7.25–7.22(m, 1H), 7.00–6.98 (m, 1H), 6.91(d, J = 8.4 Hz, 1H), 4.51–4.48(m, 2H), 4.45–4.22(m, 2H), 2.02(s, 3H), 1.41(s 9H); ^{13}C NMR (100 MHz, $CDCl_3$)δ(ppm): 171.05, 164.49, 163.79, 160.17, 153.42, 142.11, 133.50, 133.12, 132.07, 131.39, 129.90, 128.79, 127.72, 126.63, 124.21, 122.51, 116.03, 110.78, 61.71, 38.98, 34.84, 30.42, 20.89; TOF-MS: m/z: 432.1826 (M+1), Calc. for M_W: 432.1811.

2.2.7. 4-[2,4-di(tert-butyl)]phenoxy-N-(2-hydroxyethyl)-1,8-naphthalimide (3d)

Compound 3d was synthesized with the same procedure as 3c, using 2,4-di(*tert*-butyl)phenol and 2 as starting materials. Yield: 51.0%, Mp: 160–162 °C. ^{1}H NMR (400 MHz, $CDCl_3$)δ(ppm): 8.76–8.74 (m, 1H), 8.70–8.68 (m, 1H), 8.48 (d, J = 8.4 Hz, 1H), 7.81 (t, J = 8.4 Hz, 1H), 7.54 (s, 1H), 7.30–7.27 (m, 1H), 6.93 (t, J = 8.4 Hz, 2H), 4.47 (t, J = 5.2 Hz, 2H), 3.98 (t, J = 5.2 Hz, 2H), 1.38 (d, J = 9.2 Hz, 18H); ^{13}C NMR (100 MHz, $CDCl_3$)δ(ppm): 165.35, 164.77, 160.58, 150.77, 148.32, 141.09, 133.44, 132.20, 129.87, 129.01, 126.57, 124.92, 124.56, 124.10, 122.38, 121.45, 115.64, 110.62, 62.06, 42.77, 34.99, 34.80, 31.55, 30.50; TOF-MS: m/z 446.2299 (M+1), Calc. for M_W: 446.2331.

2.2.8. 4-[2,4-di(tert-butyl)]phenoxy-N-(2-acetoxyethyl)-1,8-naphthalimide (4d)

Compound 4d was synthesized with the same procedure as 4a, using 3d and acetic anhydride as starting materials. Yield: 53.0%, Mp: 108–109 °C. ^{1}H NMR(400 MHz, $CDCl_3$)δ(ppm): 8.67(d, J = 8.4 Hz, 1H), 8.61(d, J = 7.6 Hz, 1H), 8.40(d, J = 8.4 Hz, 1H), 7.73(t, J = 8.4 Hz, 1H), 7.46(s, 1H), 7.22–7.20(m, 1H), 6.88–6.83(m, 2H), 4.42(t, J = 5.2 Hz, 2H), 4.36(t, J = 5.2 Hz, 2H), 1.95(s, 3H), 1.32(d, J = 12.4 Hz, 18H); ^{13}C NMR (100 MHz, $CDCl_3$)δ(ppm): 169.98, 163.47, 162.78, 159.35, 149.82, 147.21, 140.04, 132.13, 130.97, 128.86, 127.79, 125.49, 123.85, 123.50, 123.14, 121.43, 120.36, 114.74, 109.60, 60.68, 37.92, 33.96, 33.75, 30.51, 29.46, 19.85; TOF-MS: m/z: 488.2374 (M+1), Calc. for M_W: 488.2437.

3. Results and discussion

3.1. Synthesis and characterization

All the target dyes are synthesized *via* nucleophilic substitutions of phenol derivatives with 4-bromo-1,8-naphthalimides, and the nucleophilicity of the phenols would have strong effect on the reaction conditions. For example, 3a and 3b can be prepared using K_2CO_3 as base with good yields, while 3c and 3d could not be obtained with satisfied yields until more alkaline KOH is used, because the nucleophilic reagents of 2-*tert*-butylphenol and 2,4-di (*tert*-butyl)phenol have more steric hindrance compared to phenol and 4-*tert*-butylphenol.

The chemical structures of the resulting naphthalimides are confirmed by ^{1}H NMR, ^{13}C NMR and high resolution TOF-MS spectra. All the molecules have good solubility in common organic solvents such as dichloromethane, chloroform, tetrahydrofuran,

Table 1
UV–vis absorption, photoluminescence, and melting point data of the target naphthalimides.

Compound	Melting point (°C)	In solution				In film			
		λ_{abs} (nm)[a]	λ_{PL} (nm)[a]	φ_{PL}[b]	FWHM (nm)	λ_{abs} (nm)	λ_{PL} (nm)	φ_{PL}[c]	FWHM (nm)
3a	157–158	366	429	0.55	71	369	478	0.14	95
4a	177–178	365	425	0.82	67	367	473	0.15	92
3b	174–175	369	435	0.27	67	369	471	0.42	99
4b	154–155	367	429	0.46	73	368	475	0.11	91
3c	208–210	369	432	0.66	69	369	448	0.04	76
4c	96–98	364	427	0.46	68	366	438	0.04	61
3d	167–168	374	444	0.02	65	369	451	0.29	72
4d	128–129	372	442	0.03	66	370	441	0.24	74

[a] Solution in 10^{-5} mol L^{-1} $CHCl_3$.
[b] φ_{PL} is relative PL quantum efficiency of naphthalimide solution in 10^{-5} mol L^{-1} $CHCl_3$ which is determined by using 10^{-5} mol L^{-1} quinine sulfate in 0.1 mol L^{-1} H_2SO_4 ($\varphi = 0.55$) as the standard reference.
[c] φ_{PL} is absolute PL quantum efficiency of naphthalimide solid film, which is determined with an integrating sphere together with a digital photometer.

chlorobenzene, dioxane and toluene. The melting points data of the eight molecules determined by DSC are summarized in Table 1, the results indicate that most of them have high melting points of >150 °C.

3.2. Photophysical properties

The photophysical characteristics of the objective molecules are investigated in dilute $CHCl_3$ solutions (10^{-5} mol L^{-1}) and thin solid films as well. The data of UV–vis absorption and PL emission peaks are summarized in Table 1.

3.2.1. UV–vis absorption properties

The UV–vis absorption spectra of the objective dyes are shown in Fig. 2 (in 10^{-5} mol L^{-1} $CHCl_3$ solution) and Fig. 3 (in solid films). It can be observed that the eight compounds have quite similar UV–vis absorption characteristics. The maximum absorption peaks (λ_{abs}), which can be assigned to the π-π^* electronic transitions, situate in 364–374 nm both in solution and solid films. Compared with the objective molecules, intermediate 2 has its λ_{abs} located in 340 nm with a shoulder peak of 354 nm, implying the replacement of electron-withdrawing bromo-substituent with electron-donating phenoxy groups would result in prolonged conjugation length. The resembled absorption spectra of the dyes indicate that the incorporation of *tert*-butyl with phenoxy groups would has limited effect on their electronic energy levels. But one point should be noted is that compounds 3d and 4d, which both have two *tert*-butyl modified phenoxy groups, show more red-shifted λ_{abs} of 374 nm and 372 nm in solution, giving evidence that *tert*-butyl acts as weak electron-donating substituent here.

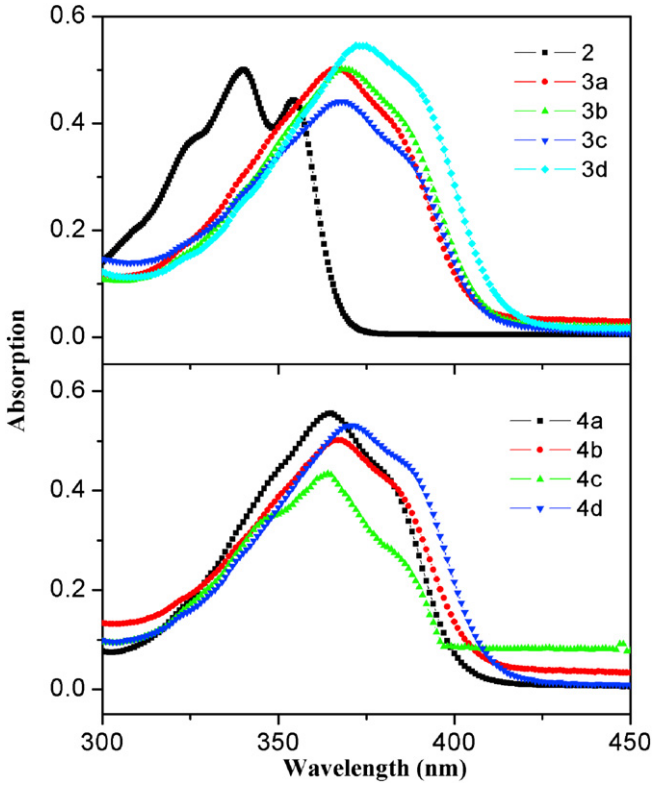

Fig. 2. UV–vis absorption spectra of 2, 3a–3d and 4a–4d in 10^{-5} mol L^{-1} $CHCl_3$ solution.

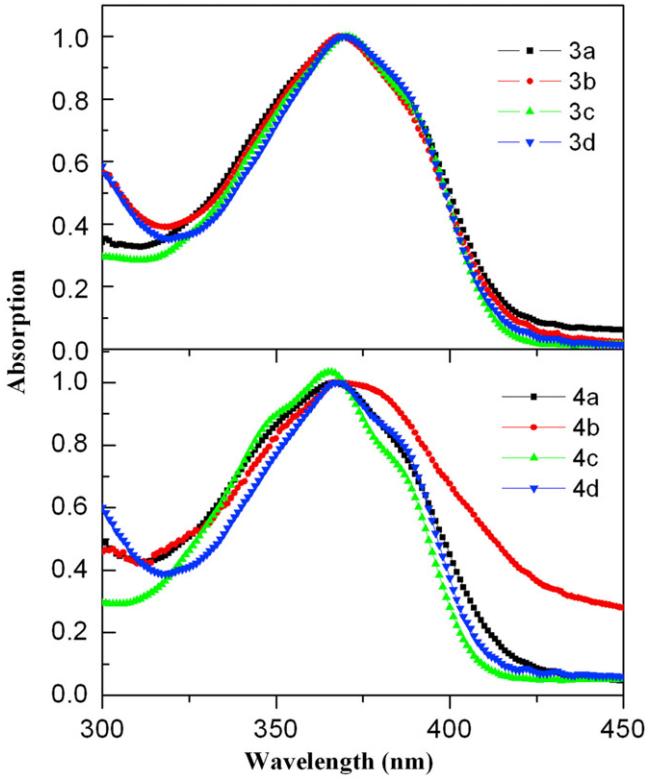

Fig. 3. UV–vis absorption spectra of 3a–3d and 4a–4d in thin solid film state.

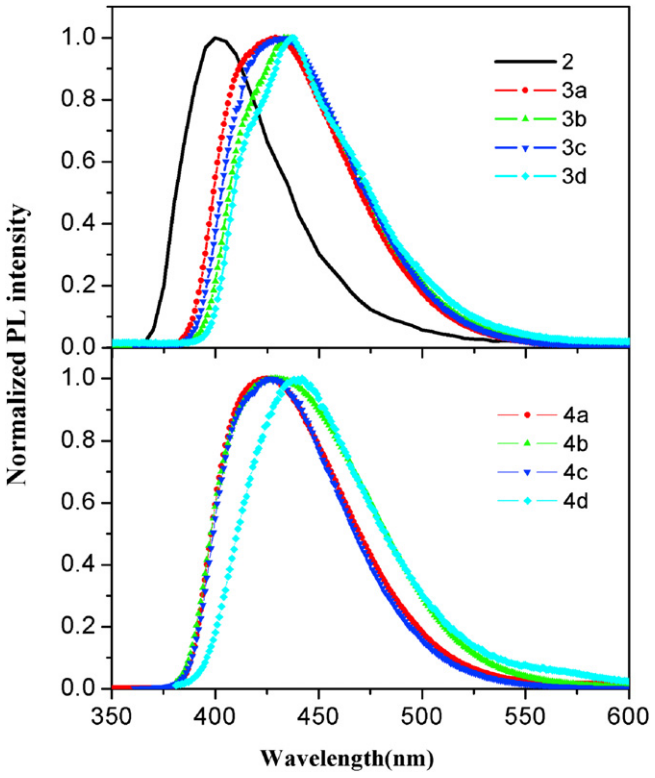

Fig. 4. PL spectra of 2, 3a–3d and 4a–4d in 10^{-5} mol L^{-1} $CHCl_3$ solution ($\lambda_{exc} = 340$ nm for 2, and $\lambda_{exc} = 376$ nm for 3 and 4).

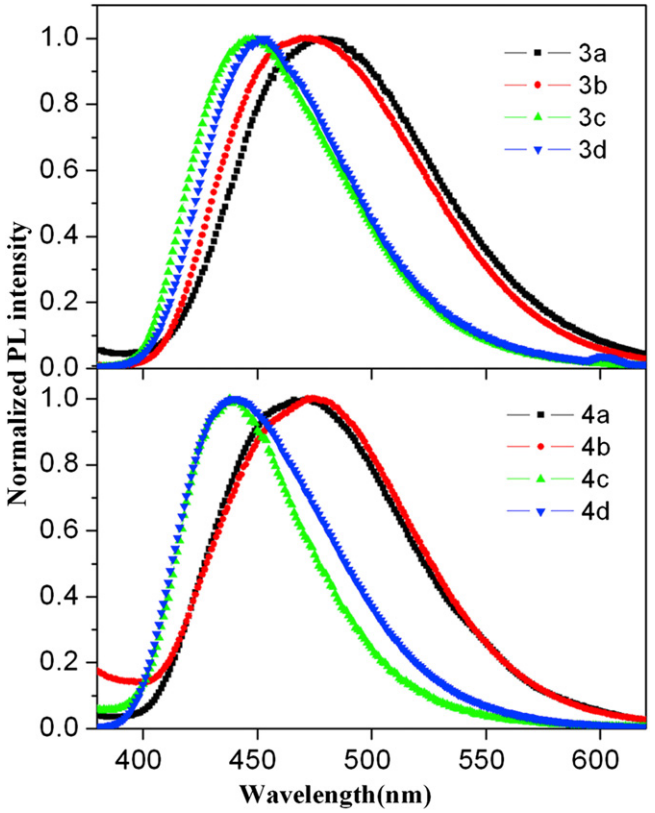

Fig. 5. PL spectra of 3a–3d and 4a–4d in thin solid film state ($\lambda_{exc} = 370$ nm).

3.2.2. Photoluminescence properties

The PL spectra of the target molecules in 10^{-5} mol L^{-1} $CHCl_3$ solution and neat films are shown in Fig. 4 and Fig. 5, respectively, PL quantum yield (φ_{PL}) data of solution and films are tabulated in Table 1. Upon UV photoexcitation, intermediate 2 exhibits quite weak PL in solution owing to the existence of the electron-withdrawing bromo-substituent, and the maximum emission peak (λ_{PLmax}) locates at 406 nm. While the replacement of bromo- with electron-donating phenoxy-substituents results in dramatically improved PL intensity due to the formation of typical D-π-A molecular structures, the emission colour is red-shifted to pure blue with λ_{PLmax} of 425–444 nm and narrow full width at half maximum (FWHM) of 65–73 nm. The fluorescence properties in solid films, however, differ from those in solution due to the condensing aggregation. Intrinsic relationships between molecular structure and PL properties have been investigated in detail.

Compounds 3a and 4a with planar phenoxy at 4-position show pure blue PL in solution ($\lambda_{PLmax} < 430$ nm), with high PL efficiencies of 0.55 and 0.82. While in solid films, the two compounds show dramatically bathochromic shifted (~50 nm) λ_{PLmax} of 478 nm and 473 nm, with much broadened FWHM of >90 nm, and the emission colour is greenish blue. Meanwhile, 3a and 4a have much lower φ_{PL} (<0.15) in solid films. These results confirm that there exists intense intermolecular aggregation and stacking in condensed states of 3a and 4a, due to their relatively planar structures.

Compounds 3b and 4b, which have *para-tert*-butylphenoxy groups, also give pure blue PL in solution, but their φ_{PL} drop greatly to 0.27 and 0.46, this can be ascribed to the free rotation of *tert*-butyl groups that quenches the singlet excited states of the fluorescent molecules [36]. Their PL emission peaks and colours in solid films are similar with those of 3a and 4a, yet the φ_{PL} of 3b is as high as 0.42, suggesting that the introduction of 4-(*para-tert*-butylphenoxy) to naphthalimide skeleton is an effective way for diminishing concentration quenching, but has limited effect on the tuning of emission colour.

By altering the *para-tert*-butyl substituents to *ortho*-ones, the resulting compounds, 3c and 4c, show pure blue PL both in solution and solid films with $\lambda_{PLmax} < 450$ nm and relative narrow FWHM of 61–76 nm. This can be attributed to the twist of phenyl-*O*-naphthalimide conjugation backbone caused by the bulky *ortho-tert*-butyl, which would result in more rigid non-planar molecules with less conjugation lengths. The rigid structures would bring about good φ_{PL} in solution, but poor φ_{PL} in condensed state due to the partly interrupted conjugation system. The experiment results are consistent with our hypothesis: the φ_{PL} of 3c and 4c are good (0.46–0.66) in solution, while as low as 0.04 in films.

The introduction of another *para-tert*-butyl into 3c and 4c gives compounds 3d and 4d. They have longer λ_{PLmax} of 444 nm and 442 nm in $CHCl_3$ solution compared to that of the other six compounds, confirming that they have longer conjugation systems, which is in accordance with the UV–vis absorption characteristics. Like 3c and 4c, 3d and 4d also give pure blue PL both in solution and solid films, but have much dropped φ_{PL} (<0.03) in solution which may be ascribed to the free rotation of *tert*-butyl groups, and much improved φ_{PL} of >0.24 in films which can be assigned to the effective inhibition of concentration quenching.

Additionally, 4a, 4b and 4d have better φ_{PL} compared to 3a, 3b and 3d, respectively, implying that the end capping of hydroxy group by acetylation may be beneficial to the enhancement of φ_{PL} in $CHCl_3$ solution.

3.2.3. Electrochemical properties

To gain information on the charge injection capabilities, the electrochemical behavior of the target dyes was investigated by cyclic voltammetry in 1 mmol L^{-1} acetonitrile solutions. As

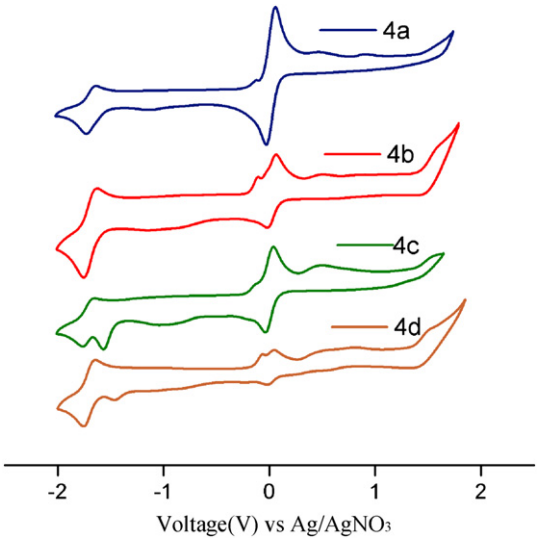

Fig. 6. Cyclic voltammograms of 4a–4d in 1 mmol L^{-1} CH_3CN solution on Pt containing 0.1 mol L^{-1} of Bu_4NPF_6 as supporting electrolyte and ferrocene/ferrocenium as calibrant, referenced with $Ag/AgNO_3$ electrode.

compounds 3a–3d all have free hydroxy groups which may form hydrogen bonds with the solvent, herewith, only the cyclic voltammograms (CV) of the four acetyl-end-capped dyes, *i.e.*, 4a–4d, are given (shown in Fig. 6). All the four compounds exhibit quasireversible reduction waves upon the cathodic sweeps, with onset reduction potentials of −1.51 ~ −1.56 V vs $Ag/AgNO_3$, while the oxidation processes exhibit irreversible waves when sweep anodically, the onset potentials of oxidation for the dyes are located at 1.33–1.43 V vs $Ag/AgNO_3$. The HOMO and LUMO energy levels of the target molecules can be estimated from the following equations [37]:

$$\text{HOMO} = (-4.8 - E^{ox}_{onset}(\text{vs Fc/Fc}^+))\text{eV}$$

$$\text{LUMO} = (-4.8 - E^{red}_{onset}(\text{vs Fc/Fc}^+))\text{eV}$$

where the constant −4.8 is the energy level of ferrocence related to the vacuum level, and E^{ox}_{onset} (vs Fc/Fc^+)/E^{red}_{onset} (vs Fc/Fc^+) are oxidation/reduction potentials relative to an $Ag/AgNO_3$ reference electrode after calibration using ferrocene/ferrocenium (Fc) redox system [38]. Table 2 outlines the onset oxidation and reduction potentials, energy levels, and the band gaps of naphthalimides 4a–4d. The results indicate that 4a–4d have low-lying LUMO energy levels ranging from −3.29 to −3.24 eV, and HOMO energy levels ranging from −6.26 to −6.16 eV, suggesting they have high electron affinities, and are potentially electron-transporting or hole-blocking blue electroluminescent materials. Their electrochemical band gaps (E^{ec}_g), calculated from cyclic voltammetry data ($E^{ox}_{onset} - E^{red}_{onset}$), are 2.95–3.01 eV, somewhat in good accordance with the optical band gaps (E^{opt}_g) estimated from the onset absorption wavelength (λ_{onset}) of the solution (3.03–3.08 eV).

Table 2
Electrochemical potentials, energy levels, and band gaps of the naphthalimides 4a–4d.

Compound	E^{ox}_{onset} vs E_{fc}(V)[a]	E^{red}_{onset} vs E_{fc}(V)[a]	HOMO (eV)	LUMO (eV)	E^{ec}_g (eV)[b]	E^{opt}_g (eV)[c]	λ_{onset} (nm)[d]
4a	1.45	−1.51	−6.25	−3.29	2.96	3.08	402
4b	1.46	−1.55	−6.26	−3.25	3.01	3.06	405
4c	1.36	−1.56	−6.16	−3.24	2.92	3.08	402
4d	1.39	−1.56	−6.19	−3.24	2.95	3.03	409

[a] E^{ox}_{onset} and E^{red}_{onset} are measured vs. ferrocene/ferrocenium.
[b] $E^{ec}_g = (E^{ox}_{onset} - E^{red}_{onset})$.
[c] E^{opt}_g stand for the band gap energy estimated from the onset wavelength of the optical absorption.
[d] λ_{onset} stand for the onset wavelength of the optical absorption spectra in chloroform solution.

4. Conclusion

By introducing phenoxy or *tert*-butyl modified phenoxy into their 4-positions, and incorporation of *N*-(2-hydroxyethyl) or *N*-(2-acetoxyethyl) substituents with their carboximide sites, eight blue light-emitting 1,8-naphthalimides are prepared, and the relationships between molecular structures and photophysical properties are investigated. The results indicate that the compounds comprising 2-(*tert*-butyl)phenoxy substituent would give pure blue PL emission in solid films, and the addition of an extra 4-(*tert*-butyl) would lead to enhanced PL quantum yield in film. The resulting compound, 4-[2,4-di(*tert*-butyl)]phenoxy-*N*-(2-hydroxyethyl)-1,8-naphthalimide, has λ_{PLmax} of ~450 nm and high φ_{PL} of 0.29, which is suitable as emitting material for fabrication of non-doping blue OLEDs. Moreover, all these compounds exhibit pure blue PL emission in chloroform solution with the highest φ_{PL} of 0.82, yet the introduction of 4-[2,4-di(*tert*-butyl)phenoxy] substituents would lower the φ_{PL} in solution. Electrochemical measurements indicate that the objective compounds have high electron affinities of 3.29–3.24 eV, implying they have good electron injection capabilities. All these results suggest that these novel naphthalimides are perspective blue dopants or non-doping blue light emitters with good electron-transporting properties for fabrication of blue OLEDs.

Acknowledgements

This work was financially supported by the National Natural Science Foundation of China under project No. 20672076.

References

[1] Okumoto K, Kanno H, Hamaa YJ, Takahashi H, Shibata K. Green fluorescent organic light-emitting device with external quantum efficiency of nearly 10%. Applied Physics Letters 2006;89:063504.
[2] Chen JS, Ma DG. Improved color purity and efficiency by a coguest emitter system in doped red light-emitting devices. Journal of Luminescence 2007;122–123:636–8.
[3] Tong QX, Lai SL, Chan MY, Zhou YC, Kwong HL, Lee CS, et al. Highly efficient blue organic light-emitting device based on a nondoped electroluminescent material. Chemistry of Materials 2008;20:6310–2.
[4] Moorthy JN, Venkatakrishnan P, Huang DF. Blue light-emitting and hole-transporting amorphous molecular materials based on diarylaminobiphenyl-functionalized bimesitylenes. Chemical Communication 2008;18:2146–8.
[5] Jou JH, Chiang PH, Lin YP, Chang CY, Lai CL. Hole-transporting-layer-free high-efficiency fluorescent blue organic light-emitting diodes. Applied Physics Letters 2007;91:043504.
[6] Park JW, Kim YH, Jung SY, Byeon KN, Jang SH, Lee SK, et al. Efficient and stable blue organic light-emitting diode based on an anthracene derivative. Thin Solid Film 2008;516:8381–5.
[7] Yao YS, Zhou QX, Wang XS, Wang Y, Zhang BW. A DCM- type red- fluorescent dopant for high-performance organic electroluminescent devices. Advanced Functional Materials 2007;17:93–100.
[8] Gao ZQ, Mi BX, Chen CH, Cheah KW, Cheng YK, Wen WS. High-efficiency deep blue host for organic light-emitting devices. Applied Physics Letters 2007;90:123506.
[9] Gong JR, Wan LJ, Lei SB, Bai CL, Zhang XH, Lee ST. Direct evidence of molecular aggregation and degradation mechanism of organic light-emitting diodes under joule heating: an STM and photoluminescence study. Journal of Physical Chemistry B 2005;109:1675–82.
[10] Mei CY, Tu GL, Zhou QG, Cheng YX, Xie ZY, Ma DG, et al. Green electroluminescent polyfluorenes containing 1,8-naphthalimide moieties as color tuner. Polymer 2006;47:4976–84.

[11] Kukhta A, Kolesnik E, Grabchev I, Sali S. Spectral and luminescent properties and electroluminescence of polyvinylcarbazole with 1,8-naphthalimide in the side chain. Journal of Fluorescence 2006;16:375–8.
[12] Ding GH, Xu ZW, Zhong GY. Synthesis, photophysical and electroluminescent properties of novel naphthalimide derivatives containing an electron-transporting unit. Research on Chemical Intermediates 2008;34(2–3): 299–308.
[13] Liu J, Cao JX, Shao SY, Xie ZY, Cheng YX, Geng YH, et al. Blue electroluminescent polymers with dopant-host systems and molecular dispersion features: polyfluorene as the deep blue host and 1,8-naphthalimide derivative units as the light blue dopants. Journal of Materials Chemistry 2008;18(14):1659–66.
[14] Islam A, Cheng CC, Chi SH, Lee SJ, Hela GP, Chen IC, et al. Aminonaphthalic anhydrides as red-emitting materials: electroluminescence, crystal structure, and photophysical properties. Journal of Physical Chemistry B 2005;109: 5509–17.
[15] Bojinov V, Ivanova G, Chovelon JM, Grabchev I. Photophysical and photochemical properties of some 3-bromo-4-alkylamino-*N*-alkyl-1,8-naphthalimides. Dyes and Pigments 2003;58:65–71.
[16] Distanov VB, Berdanova VF, Stepanenko AA, Prezhdo VV. Influence of triphenylphospine complex on condensation of acetylenes with aryl halides. Dyes and Pigments 1997;35(2):183–9.
[17] Yang JX, Wang XL, Wang XM, Xu LH. The synthesis and spectral properties of novel 4-phenylacetylene-1,8-naphthalimide derivatives. Dyes and Pigments 2005;66:83–7.
[18] Yang JX, Wang XL, Tu S, Xu LH. Studies on the synthesis and spectral properties of novel 4-benzofuranyl-1,8-naphthalimide derivatives. Dyes and Pigments 2005;67:27–33.
[19] Magalhaes JL, Pereira RV, Triboni ER, Berci Filho P, Gehlen MH, Nart FC. Solvent effect on the photophysical properties of 4-phenoxy- *N*-methyl-1,8-naphthalimide. Journal of Photochemistry and Photobiology A: Chemistry 2006;183:165–70.
[20] Cacialli F, Friend RH, Bouche CM, Le Barny P, Facoetti H, Soyer F, et al. Naphthalimide side-chain polymers for organic light-emitting diodes: band-offset engineering and role of polymer thickness. Journal of Applied Physics 1998;83:2343–56.
[21] Hu C, Zhu WH, Lin WQ, Tian H. Synthesis and luminescence of novel emitting copolymers. Synthetic Metals 1999;102:1129–30.
[22] Zhu WH, Hu M, Wu YQ, Tian H, Sun RG, Epstein AJ. Novel luminescent carbazole-naphthalimide dyads for single-layer electroluminescent device. Synthetic Metals 2001;119:547–8.
[23] Tian H, Su JH, Chen KC, Wong TC, Gao ZQ, Lee CS, et al. Electroluminescent property and charge separation state of bis-naphthalimides. Optical Materials 2000;14:91–4.
[24] Tian H, Zhu W, Chen KC. Novel triad luminescent compound with an electron transporting and a hole transporting moiety. Synthetic Metals 1997; 91:229–31.
[25] Liu J, Min CC, Zhou QG, Cheng YX, Wang LX, Ma DG, et al. Blue light-emitting polymer with polyfluorene as the host and highly fluorescent 4-dimethylamino-1,8-naphthalimide as the dopant in the sidechain. Applied Physics Letters 2006;88:083505.
[26] Wang S, Zeng PJ, Liu YQ, Yu G, Sun XB, Niu HB, et al. Luminescent properties of a novel naphthalimide-fluorene molecule. Synthetic Metals 2005; 150:33–8.
[27] Gan JA, Song QL, Hou XY, Chen KC, Tian H. 1,8-Naphthalimides for non-doping OLEDs: the tunable emission color from blue, green to red. Journal of Photochemistry and Photobiology, A: Chemistry 2004;162:399–406.
[28] Yang JX, Wen JX, Xu LH. The studies of synthesis and electroluminescence of 4-phenylethynyl-1,8-naphthalimides. Chinese Journal of Luminescence 2007;28(4):498–504.
[29] Mikroyannidisa JA, Ye SH, Liu YQ. Electroluminesent divinylene- and trivinylene-molecules with terminal naphthalimide or phthalimide segments. Synthetic Metals 2009;159:492–500.
[30] Georgiev NI, Bojinov VB, Nikolov Peter S. Design and synthesis of a novel pH sensitive core and peripherally 1,8-naphthalimide-labeled PAMAM dendron as light harvesting antenna. Dyes and Pigments 2009; 81:18–26.
[31] Adachi C, Tsutsui T, Saito S. Blue light-emitting organic electroluminescent devices. Applied Physics Letters 1990;56(9):799–801.
[32] Chiaki H, Yamashita M. Naphthalimides. JP 39009280.
[33] Sun J, Yuan AL, Wang HB, Sun J. *N*-(2-Hydroxyethyl)-1,8-naphthalimide. Acta Crystallographica Section E Structure Reports Online 2009;E65:o1210.
[34] Wu FI, Shu CF, Chien CH, Tao YT. Fluorene-based oxadiazoles: thermally stable electron-transporting materials for light-emitting devices. Synthetic Metals 2005;148:133–9.
[35] Grayshan PH, Kadhim AM, Peters AT. Heterocyclic derivatives of naphthalene-1.8-dicarboxylic anhydride. Part III. Benzo[k, l]thioxanthene-3,4-dicarboximides. Journal of Heterocyclic Chemistry 1974;11(1):33–8.
[36] Zheng M, Sarker AM, Gurel EE, Lahti PM, Karasz FE. Structure-property relationships in light-emitting polymers: optical, electrochemical, and thermal studies. Macromolecules 2000;33:7426–30.
[37] Zhong HP, Zhe NB, Mary EG. Polymers with bipolar carrier transport abilities for light emitting diodes. Chemistry of Materials 1998;10:2086–90.
[38] Kang JW, Lee DS, Park HD, Park YS, Kim JW, Jeong WI, et al. Silane- and triazine- containing hole and exciton blocking material for high-efficiency phosphorescent organic light emitting diodes. Journal of Material Chemistry 2007;17:3714–9.